NISS

Random-Walk-Based Estimates of Transport Properties in Small Specimens of Composite Materials

Jeffrey D. Picka and Karthik Chermakani

Technical Report Number 119
October, 2001

National Institute of Statistical Sciences
19 T. W. Alexander Drive
PO Box 14006
Research Triangle Park, NC 27709-4006
www.niss.org

Random-Walk-Based Estimates of Transport Properties in Small Specimens of Composite Materials

Jeffrey D. Picka*

National Institute of Statistical Sciences

and Department of Mathematics, University of Maryland, College Park MD

Karthik Chermakani

Microsoft Corp., Redmond WA

(Dated: October 19, 2001)

Abstract

A method based on random walks is developed for estimating the DC conductance and similar transport properties in small specimens of composite materials. The method is valid over a much wider range of material structures than are asymptotic methods, and requires only that the internal structure of the material be known. The error in its estimates is limited primarily by CPU speed. It is found to work best for composites consisting of a bulk conducting phase and inclusions of lower conductivity.

PACS numbers: 05.60.Cd, 46.65.+g, 02.60, 74.25.Fy

* jdp@math.umd.edu; http://www.math.umd.edu/~jdp

I. INTRODUCTION

Given a conductor that contains many small inclusions of a second phase with a different conductivity, Maxwell [1] established that the dependence of composition conductivity on the conductivities of the components can be approximated by a non-trivial function of the volume fractions of each component in the material. If the specimen is very large, if one phase consists of monosized spheres randomly dispersed within the other phase, if the spheres are distributed uniformly and isotropically in space, and if they are spaced far enough apart so that the influences of neighboring spheres upon the potential field in the continuous phase are independent of each other, then the approximate conductivity of the composite $\widehat{\sigma}_c$ is

$$\frac{\widehat{\sigma}_c}{\sigma_0} = \frac{2\sigma_0 + \sigma_1 - 2p(\sigma_0 - \sigma_1)}{2\sigma_0 + \sigma_1 + p(\sigma_0 - \sigma_1)} \tag{1}$$

where p is the volume fraction of inclusions, σ_0 is the conductivity of the continuous phase, and σ_1 is the conductivity of the dispersed phase. This approximation is appealing in applications, as it is not conditional on any specific details of the internal structure of the material. Further, it can be generalized to any other steady-state transport process that can be modeled by the same type of elliptical PDE and boundary conditions as DC electrical conduction, including electrical permittivity, magnetic permeability, thermal conductivity, and diffusivity [2].

If a specimen of composite is small, in the sense that it contains tens rather than thousands of inclusions, then the derivation of Maxwell's result is no longer applicable and asymptotic expressions for material properties may no longer be reliable. Methods are needed for efficiently estimating small specimen conductance, and these can be found through the use of statistics based upon random walks.

A. Asymptotic Methods

Asymptotic methods for estimating composite conductivity [3, 4] use the large scale average properties of disordered composites in order to find approximate relationships between the composite conductivity σ_c and σ_1, σ_0, p, and other material properties. These approximations may be in the form of functional estimates, or in the form of bounds.

If the inclusions in a material are arranged in a cubic order, then Rayleigh [5] demonstrated that (1) also describes the effects of an infinite cubic array of spherical inclusions on the conductivity of a composite, when the volume fraction p of spheres is small. Rayleigh's analysis also included extra terms that accommodated interactions between the electric field and pairs of neighboring inclusions, making use of the symmetry in the problem to make the analysis tractable. This analysis was later corrected [6], made fully rigorous [7–9], and extended to spheroidal inclusions [10]. One asymptotic approximation that applies to mono-sized discs in the plane (or aligned infinite cylinders in space) [11] is

$$\frac{\sigma_c}{\sigma_0} = 1 - \frac{2p}{T + p - \frac{0.305827 p^4 T}{T^2 - 1.402958 p^8} - \frac{0.013362 p^8}{T}} \tag{2}$$

where

$$T = \frac{\sigma_0 - \sigma_1}{\sigma_0 + \sigma_1}.$$

The ordered sphere model is useful in that its asymptotics can be rigorously derived from the geometric structure of the inclusions, which can also be easily simulated.

For materials in which the inclusions are disordered, asymptotic methods that improve upon Maxwell's result have been developed. The effective medium theories [12–14] provide asymptotic approximations that are closely related to coherent potential and average t-matrix approximations from quantum scattering theory [15]. Bounds can also be found for the composite conductivity, and Hashin and Shtrikman [16] have shown that Maxwell's equation is the best upper bound that can be found that is a function only of phase conductivities and inclusion volume fraction. Improvements in these bounds are made by making them functions of n-point correlations [17–20]. These correlations, known in probability theory as the n^{th} moments of the realization of a random set [21, 22], describe the the average properties of the random structure of inclusions. Their use also requires the assumption that the random pattern of inclusions is stationary, and thus of infinite extent.

In applications, it is often difficult to make an *a priori* decision about which asymptotic approximation will best describe experimental data. As a consequence, practitioners often try many different asymptotic models before finding one that fits [23–27]. In the case of dilute oil/water emulsions [24], the unsymmetric effective medium equation provides an excellent fit, but fails to adequately describe the conductivity of dog's blood as a function of red cell concentration [28]. In the latter case, a modification of Maxwell's equation that adjusts for the non-spherical shape of red blood cells [29] performs much better. In solid phase studies of dielectric properties of sintered UO_2 powders [30], Maxwell's equation fits the data well, while in studies of aluminum powder-epoxy resin composites [31], effective medium equations provide better fits. Four reasons that these difficulties may arise are as follows.

1. The assumptions made in deriving asymptotic approximations may be difficult to relate to the physical structure of the material. For example, it takes considerable effort to find a material for which the symmetric effective medium theory acts as a coherent potential approximation for overall material conductivity [32].

2. The assumptions made in deriving asymptotic approximations are often valid only in the dilute limit (i.e. $p \leq 0.2$). In the case of ordered inclusions, symmetry can be used to extend these to much higher volume fractions.

3. The model for the transport process may not be complete. For example, failure to account for frequency-dependent aspects of permittivity can produce errors in experimental studies [33, 34].

4. The specimen may be too small for the asymptotic arguments to apply, and the local variability of its properties may not be averaged away. Further, there may be boundary effects that cannot accounted for in the asymptotic arguments, or the specimen may fail to be stationary or isotropic in other ways.

B. Estimating Conductivity in Large Samples

The conductivity of large samples can be estimated through simulation routines based upon the Einstein correspondence between diffusivity and random walks [35]. In the ant-in-the labyrinth algorithm [36, 37], points are randomly chosen within a conductive phase of a composite. Each of these points is used as the starting point for a simple random walk with fixed step length and randomly chosen orientation at each step, which is used to simulate a diffusion. When the random walk hits an inclusion, its step length changes if the inclusion is conducting, and the walk stops at the surface if the inclusion is insulating. The walk is run for a fixed number of time steps, and the average Euclidean distance traveled is proportional to the diffusivity of the composite.

For smaller specimens of composite, this algorithm cannot be used. There will be a significant probability that the random walk will encounter a specimen boundary, unless the walk is restricted to beginning far from any boundaries. If the dispersed phase is not uniformly distributed, then a walk that avoids parts of the sample may generate biased estimates of specimen conductance.

II. METHODS FOR SMALL SAMPLES

For this and further sections, the transport property considered will be DC conduction. The specimen whose conductance is to be estimated is a square region D in $\mathbb{R}^2$ with sides of unit length. This boundary is divided into four parts (Figure 1): the side A_1 through which the current enters, the opposite side A_0 through which the current leaves, and two insulated sides S_1 and S_2 through which no current may pass. Any inclusions will be assumed to have boundaries that are Lipschitz-continuous functions, and so do not possess too many corners or very rough sections. If the inclusions have random size, it will be assumed that there is a fixed minimum size. The n inclusions present are designated $B_1, \ldots, B_n$. The inclusion conductivity is $\sigma_1 \in [0, \infty)$, and the continuous phase conductivity is $\sigma_0 \in (0, \infty)$. No assumptions will be made about the arrangement of the inclusions within the specimen, except that their locations, shapes, and orientations are known.

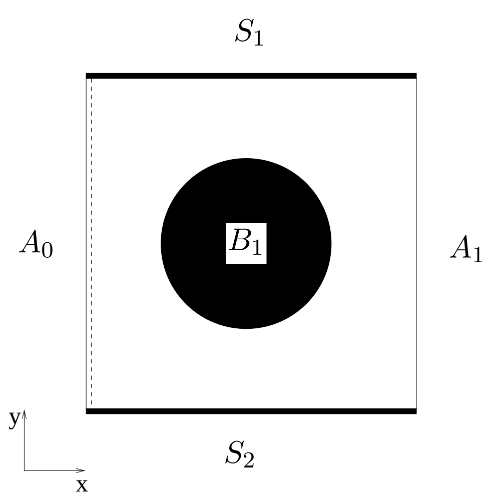

FIG. 1: The specimen considered here is a unit square in the plane. The current enters through A_1 and leaves at A_0, and the sides S_1 and S_2 are insulated. The inclusion B_1 may be insulating or conducting, but not superconducting. The dotted line is the location of the initial points for the diffusions and random walks discussed in section II C 1.

A. The Existence of a Solution

The flow of DC current through the specimen is determined by a potential ϕ, which must satisfy

$$\nabla\sigma\nabla\phi = 0 \tag{3}$$

where $\sigma : \mathbb{R}^2 \rightarrow [0,\infty)$ is an L^∞ function and the boundary conditions are

$$\phi = 1 \qquad \text{on} \quad A_1 \quad (x=1) \tag{4}$$

$$\phi = 0 \qquad \text{on} \quad A_0 \quad (x=0) \tag{5}$$

$$\frac{\partial\phi}{\partial n} = 0 \qquad \text{on} \quad S_1, S_2 \tag{6}$$

$$\sigma\frac{\partial\phi}{\partial n} \quad \text{is} \quad C^1 \quad \text{on the boundary of} \quad B_1,\ldots B_n, \tag{7}$$

where n is a normal vector to S_1, S_2, or B_i. The $B_1 \ldots B_n$ are considered to be part of the boundary if the inclusions are insulating. Since (3) is an elliptical PDE with an L^∞ coefficient and since the boundary conditions are Lipschitz, there exists a unique solution ϕ to the equation [38] which will be Hölder continuous if not twice differentiable at almost every point in the specimen [39].

If there are no inclusions, the solution will be $\phi(x,y) = x$ at any point in D. In general, the solution ϕ cannot be expressed in terms of elementary functions or power series, but it is possible to directly estimate the value of ϕ at any point using random walks on the lattice or in the plane.

B. Approximation of Conductance Using a Random Walk on A Lattice

The specimen D can be modeled discretely by a square lattice whose edges have resistances determined by the underlying material (Figure 2). If an edge lies entirely within phase i, the it is assigned conductance $\varsigma = \sigma_i$. If an edge crosses a phase boundary so that a fraction ρ of its length lies in phase i and the remainder lies in phase j, then the conductance assigned to the edge will be

$$\varsigma^{-1} = \rho\sigma_i^{-1} + (1-\rho)\sigma_j^{-1}. \tag{8}$$

If the vertex lies on an insulating edge S_i, then it has no edge crossing beyond the insulating boundary. If the point lies on A_0 or A_1, then there are no edges coincident with these surfaces, and the edge passing into them and connecting the specimen to the power source has no resistance.

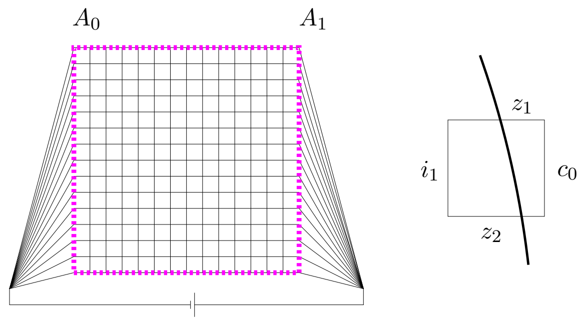

FIG. 2: At left, the lattice representation of the specimen (dotted outline) with lattice edges coincident with S_1 and S_2, and edges connected to the current source by the slanted superconducting wires. At right, the curve is the boundary of a spherical inclusion, the edge i_1 has conductance σ_1, the edge c_0 has conductance σ_0, and the edges z_1 and z_2 have conductance given by (8).

Given this discrete representation of the specimen, the methods of Doyle and Snell [40] can be used to find the effective resistance of the network. One of the edges connecting to A_1 is chosen at random, and a random walker is positioned at the corresponding vertex inside the material. The next step is taken along the i^{th} edge out of that vertex with probability $q_i = \varsigma_i / \sum_{j=1}^{4} \varsigma_j$. If the step takes the walker back to A_1, the walk ends. Otherwise, the walker continues until it either reaches A_1 or A_0. The probability that walk reaches A_0 before returning to A_1 is the escape probability of the network, and it is proportional to the effective conductance of the entire network. The ratio of escape probabilities for the discretizations of two different specimens is an estimate of their relative conductance.

Representation of a specimen by means of a discrete resistor model has been used in modeling the structure of cement paste [41]. In that case, the percolation threshold of the composite for the conducting phase was estimated, rather than the conductance. A continuous version of a resistor model has been used in studies of heat conduction [42–44], but this model assumes that the equipotential lines $\{(x, y) : \phi(x, y) = k\}$ for fixed k are straight lines, which yields biased estimates of conductance.

C. Estimation of Conductance Using a Continuous Random Walk

The discrete approximation of a specimen is slow, since the walk must proceed through the lattice one edge at a time. The interaction between the walk and the boundaries and interfaces determines the escape probability, but most of the time during the walk is expended traversing long distances through a single phase of material. The lattice can be coarsened in order to increase speed, but this increases discretization error. By using simple random walks in $\mathbb{R}^2$ rather than on a lattice, both problems can be avoided.

1. Estimating the Conductance

The relative conductance of two unit square specimens satisfies

$$\frac{\varsigma_1}{\varsigma_2} = \frac{I_1}{I_2}$$

where ς_j is the conductance of specimen j, and I_j is its current flux across the line $x = 0$, as defined by

$$I_j = \int_0^1 \sigma(\epsilon, y) \frac{\partial \phi_j}{\partial x}(\epsilon, y) dy.$$

An estimator of ς_1/ς_2 can be constructed that avoids having to estimate the derivative directly.

Assume that there are no inclusions on the line $x = \epsilon$ (see Figure 1), or in the region between A_0 and $x = \epsilon$, where ϵ is close to 0. A one-term Taylor series expansion of ϕ is

$$\begin{aligned} \phi(\epsilon, y) =& \phi(0, y) + \left(\frac{\partial \phi}{\partial x}(0, y) \right) \epsilon \\ &+ \left(\frac{\partial^2 \phi}{\partial x^2}(\xi(y), y) \right) \frac{\epsilon^2}{2} \end{aligned}$$

for some value $\xi(y) \in \{(\delta, y) : 0 \leq \delta \leq \epsilon\}$, and so

$$\begin{aligned} \int_0^1 \frac{\partial \phi}{\partial x}(0, y) dy =& \frac{1}{\epsilon} \int_0^1 \phi(\epsilon, y) dy \\ &- \frac{\epsilon}{2} \int_0^1 \frac{\partial^2 \phi}{\partial x^2}(\xi(y), y) dy. \end{aligned} \tag{9}$$

If the conductance of the specimen is being compared to an inclusion-free specimen whose potential is $\phi_0(x, y) = x$, then $\int_0^1 \frac{\partial \phi_0}{\partial x}(0, y) dy = 1$ and the relative conductance can be estimated using the leading term of (9). If the conductances of two specimens with potentials ϕ_i, $i = 1, 2$ are being compared, then

$$\frac{\varsigma_1}{\varsigma_2} = \frac{\xi_1}{\xi_2} + \epsilon^2 \left(\frac{\frac{\xi_1}{\xi_2} - \frac{R_1}{R_2}}{\frac{R_1}{R_2} - \epsilon^2} \right) \tag{10}$$

where

$$\xi_i = \int_0^1 \phi_i(\epsilon, y) dy$$

and

$$R_i = \int_0^1 \frac{\partial^2 \phi_i}{\partial x^2} (\xi_i(y), y) dy.$$

As long as the R_i are similar in magnitude, the size of the remainder term will be dominated by ϵ.

Continuous random walks can be applied to specimens in $\mathbb{R}^3$, so long as the charge enters and leaves through 2-dimensional subsets of the surface of the specimen. The specimen also need not be cubic, so long as it possesses no unusual concentrations of corners or other rough areas.

2. *Estimating the Potential*

Random walks can be used to approximate the solutions of elliptical boundary value problems if the local conductivity $\sigma(x, y)$ is a bounded measurable function [45, 46]. This is the case when inclusions and the bulk material have finite but different conductivities, but is not the case when the inclusions are superconducting.

Under the boundary conditions specified in (4-7), if (x, y) is any point in a conducting region on the interior of the specimen, then

$$\phi(x, y) = \int_{A_1} \phi(1, \xi) P_1(d\xi) + \int_{A_0} \phi(0, \xi) P_0(d\xi) \tag{11}$$

where $P_i(d\xi)$ is the probability that a Brownian motion that begins at (x, y) reaches a small neighbourhood around a point ξ on the boundary A_i before reaching any other point on A_0 or A_1. By fixing ϕ at 0 and 1 on A_0 and A_1 respectively, (11) reduces to

$$\begin{aligned} \phi(x, y) = \mathrm{Pr}\,[& \text{ Brownian motion beginning at } (x, y) \\ & \text{crosses } A_1 \text{ before crossing } A_0 \,] \end{aligned} \tag{12}$$

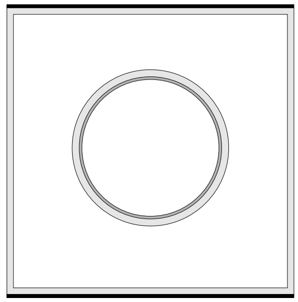

FIG. 3: On the white regions, the random walk proceeds via a walk on spheres. On the lightly shaded regions, the walk proceeds by steps of fixed length δ_0, and the regions have thickness $5\delta_0$. Within the darker shaded region, the walk proceeds by steps of length $(\sigma_1/\sigma_0)\delta_0$, where σ_1 is the inclusion conductivity and σ_0 is the continuous phase conductivity. Steps crossing the boundary between the two shaded regions have their length altered via equation (13).

This allows ϕ to be estimated at individual points in D [47, 48], unlike finite element methods that require estimation of ϕ over the entirety of D. Also, (12) shows that the integral ξ used in (9) and (10) is the mean escape probability to the surface A_1 for points randomly chosen from a uniform distribution on the line $x = \epsilon$.

3. Approximating the Brownian Motion

Realizations of a Brownian motion cannot be directly simulated, but must themselves be simulated via other stochastic processes. A combination of two different simulations is used, in order to balance the speed of execution against the need for accuracy in the crucial regions around the boundaries and interfaces in the specimen.

In the neighbourhood of boundaries and interfaces, the Brownian motion is simulated by a simple random walk, with steps of fixed length δ_i whose direction is chosen from a uniform distribution on the unit disc. The step length in the i^{th} phase is chosen to be proportional to the the conductivity σ_i of that phase. If a step intersects an insulating boundary, then the step terminates at the boundary and takes the next step that will send it free from the insulating surface. If the step crosses a boundary from a phase of conductivity σ_i to a phase of conductivity $\sigma_j > 0$ at a fraction ρ of its length, then the step length changes from δ_i to

$$\left(\rho + (1-\rho)\frac{\sigma_j}{\sigma_i}\right)\delta_i, \tag{13}$$

as justified by the arguments of Hong *et al.* [37]. The subset of phase i in D where the simple random walk is used is defined to be all points within $5\delta_i$ of a boundary or interface. For a single spherical inclusion, these neighbourhoods are shown in Figure 3.

In the remainder of D, the diffusion is simulated by using the random walk on spheres [49]. In the i^{th} phase, a sphere having diameter $2.5\delta_i$ less than the distance to the nearest boundary or interface is constructed at the end of the previous step, and the next step in the simulation is a point randomly chosen from a uniform distribution on the surface of this sphere.

Each walk begins from a point (ϵ, U) on the line $x = \epsilon$, where U is chosen from a uniform distribution on the interval $[0, 1]$. If each choice of starting point and subsequent step direction are mutually independent, then ξ is estimated by

$$\widehat{\xi} = \frac{1}{n} \sum_{i=1}^{N} \Phi_i \tag{14}$$

where each $\Phi_i \sim \text{Binomial}(1, \phi(\epsilon, U_i))$. This is an unbiased estimator when the conductance relative to the empty square specimen is estimated, since

$$\mathrm{E}[\widehat{\xi}] = \mathrm{E}[\mathrm{E}[\Phi_1 | U_1]] = \mathrm{E}[\phi(\epsilon, U_1)] = \xi.$$

III. SOURCES AND CONTROL OF ERROR

There are three main sources of error in the procedure. The control of these errors is limited by the capacity of the CPU used.

A. Errors From Approximating The Diffusion

Since the diffusion must be simulated by other stochastic processes, some error will be introduced. While this error is difficult to quantify when two simulation methods are used, its magnitude can be minimized by choosing the step size in the simple random walks to be as small as feasible. In this case, it was found that step sizes on the order of 0.00001-0.00005 worked best. These are much smaller than those recommended by Schwartz and Banavar [50], who recommended using a step size 0.01 times the diameter of the smallest inclusion.

B. Errors From Estimating the Derivative

As can be seen from the remainder terms of the derivative estimates (9, 10), the quality of $\widehat{\xi}$ as an estimator of relative conductance depends upon the linearity of $\phi(x, y)$ for fixed y in the thin strip between $x = 0$ and $x = \epsilon$. Since the relative error in this estimate will be roughly proportional to ϵ in these circumstances, taking ϵ as close to zero as feasible will yield the best results. If the equipotential lines in the strip show sharp curvature, as would be present if inclusions are close to or intersect with strip, then this is likely to introduce additional error into this estimate, and still smaller values of ϵ would be required.

C. Errors From Estimating The Potential

The error in the estimation of ξ is best expressed as the standard deviation of the estimator $\widehat{\xi}$. The variance of $\widehat{\xi}$ is given by

$$\begin{aligned} N\mathrm{Var}\,[\widehat{\xi}] &= \mathrm{E}\,[\mathrm{Var}\,[\Phi_1|U_1]] + \mathrm{Var}\,[\mathrm{E}\,[\Phi_1|U_1]] \\ &= \left(\mathrm{E}\,\left[\phi(\epsilon, U_1)\right] - \mathrm{E}\left[\phi(\epsilon, U_1)^2\right]\right) \\ &\quad + \left(\mathrm{E}\left[\phi(\epsilon, U_1)^2\right] - \mathrm{E}\left[\phi(\epsilon, U_1)\right]^2\right) \\ &= \xi\,(1 - \xi)\,, \end{aligned}$$

and so the standard deviation of $\widehat{\xi}$ is

$$\mathrm{SD}[\widehat{\xi}] = \sqrt{\frac{\xi(1-\xi)}{N}}.$$

By choosing N large, this error can be made as small as needed. Confidence intervals based on this standard deviation alone in the experiments described below indicate that the observed errors in those experiments arise primarily from the other two types of error when $N = 10^6$.

IV. SIMULATION EXPERIMENTS AND COMPARISON WITH THEORY

Two sets of simulation experiments were carried out, one based on a regular arrangement of discs and the other based on disordered arrangements.

In each case, 10^6 random walks were simulated on a Sun Ultra 10 CPU. The program was written in C, incorporating the `ran2` random number generator from Numerical Recipes

[51]. The time required is proportional to p and to the number of spheres used, for any fixed ratio of σ_1/σ_2. Each walk is allowed to take at most 50 million steps. Each data point requires between 5 and 90 hours to estimate, but this may be reducible through further refinements to the diffusion approximation (e.g. parallelization), or through acceptance of a higher error.

A. Ordered Inclusions

The conductance of a specimen whose inclusions are arranged in a centered square array within the specimen (e.g. Figure 4, left) is estimated relative to the conductance of a pure conductor specimen. Results are compared with the theoretical prediction of Perrins *et al.* (2) for $\sigma_1 < \sigma_0$ in Figure 5 and for $\sigma_1 > \sigma_0$ in Figure 6.

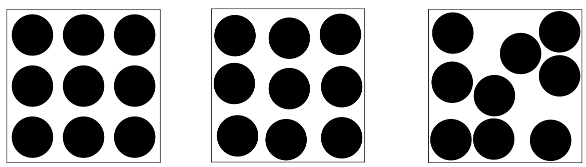

FIG. 4: From left to right: an ordered array of nine inclusions, a perturbed ordered array, and an arbitrarily arranged array. All inclusions are assumed to be insulating, and of the same size. The volume fraction of inclusion in all three specimens is $p = 0.5$.

In all cases where the inclusions are less conductive, the simulations and (2) are in very strong agreement. This could be on account of similar biases in both methods, but if this were not the case then it indicates that the asymptotic result can be used on any scale of rectangular array. The comparison of results from a single inclusion with those from a centered square array of 16 inclusions (Table I) reinforces this conclusion. Variation around the asymptotic estimate increases with inclusion conductivity, and also as the size of the inclusions is reduced.

B. Disordered Inclusions

To test the effect of inclusion position, the conductances of the disc arrangements given in Figure 4 are estimated. The first arrangement is a regular square array, the second is that

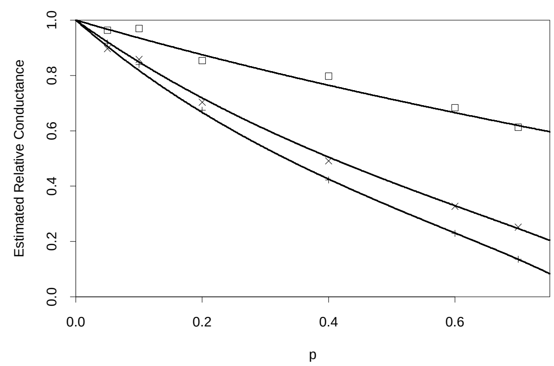

FIG. 5: Comparison of asymptotic estimates (lines, as found from (2)) with simulation estimates for specimens with a single inclusion whose conductivity satisfies $\sigma_1/\sigma_0 = 0.0$ (+), σ_1/σ_0= 0.1 (×) and σ_1/σ_0= 0.5 (□). Note that error decreases as p and σ_1/σ_0 decreases. All estimates are made relative to a specimen of pure conductor.

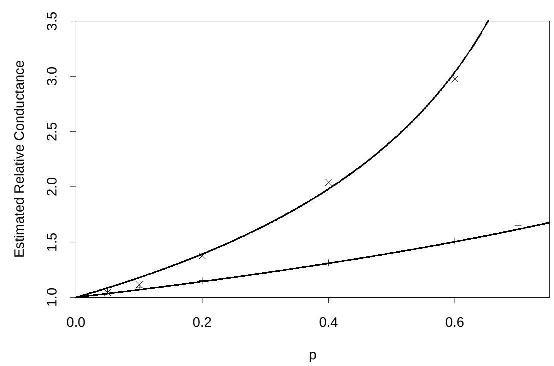

FIG. 6: Comparison of asymptotic estimates (lines, as found from (2)) with simulation estimates for specimens with a single inclusion whose conductivity satisfies $\sigma_1/\sigma_0 = 2$ (+) and σ_1/σ_0= 10 (×). Note that error decreases as p and σ_1/σ_0 decreases. All estimates are made relative to a specimen of pure conductor.

array slightly perturbed, and the third is an arbitrary arrangement. The second arrangement was prepared by dividing the specimen into a grid of 9 cells with sides of length 1/3, and the choosing the location of the centre of each inclusion from a uniform distribution on the square region that contains all possible disc locations that still lie within the cell when $p = 0.5$. In all cases, the 9 discs are of identical size.

p	Asymptotic Estimate	Simulation Estimate (1 inc.)	Simulation Estimate (16 inc.)
0.05	0.9048	0.9172	0.9048
0.1	0.8182	0.8398	0.8290
0.2	0.6667	0.6746	0.6683
0.4	0.4286	0.4225	0.4260
0.6	0.2304	0.2292	0.2286

TABLE I: Comparison of estimates based upon 1 insulating inclusion and 16 insulating inclusions.

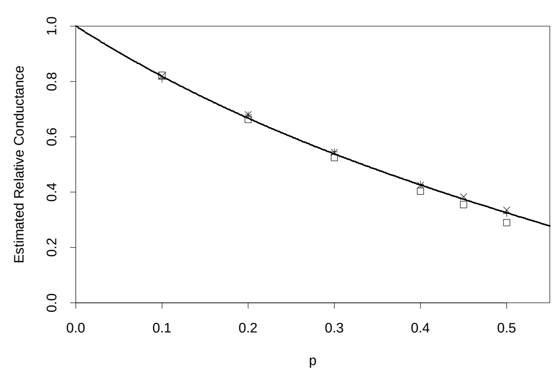

FIG. 7: Plot of the effects of inclusion arrangement on specimen conductance. All inclusions were centered at the same locations as those seen in Figure 4, and sphere radii were reduced to give other values of p. The solid line is equation (2), while the points represent simulation estimates for the ordered (+), randomly perturbed (×), and arbitrarily arranged (□) specimens.

The locations of the centres of discs in Figure 4 were used as the centres of smaller discs to obtain lower volume fractions p of inclusion. For $p \leq 0.4$, the ordered and perturbed specimens are indistinguishable from the prediction of equation (2) and from each other. For larger values of p, the perturbed specimen was slightly more conductive than expected. The arbitrarily arranged specimen was consistently less conductive than the ordered specimen, to a greater degree with increasing p. These differences are not attributed to error, as the estimates are assumed to have the same distribution around the true conductance as do the ordered specimen simulations around the prediction from (2).

V. OTHER INTERPRETATIONS OF THE METHOD

The use of escape probabilities in estimating overall conductance can be interpreted heuristically as a stochastic technique for estimating the physical properties of complex and possibly disordered structures. The continuous, conducting phase of the composite is formed by the inclusions into a network, and the overall conductance properties of this network are either enhanced or reduced by the inclusions. For the remainder, assume that the inclusions are insulators ($\sigma_1 = 0$).

If a rectangular specimen consists of a single phase, its overall conductance is proportional to its width W_i and inversely proportional to its depth d_i. Basic results from diffusion theory [52] imply that $d_i \propto \xi_i^{-1}$ when no inclusions are present, and (10) implies that

$$\frac{\varsigma_1}{\varsigma_2} \approx \frac{W_1}{W_2} \times \frac{\xi_1}{\xi_2}$$

when inclusions are present. This suggests that ξ_i^{-1} is measuring an average distance between the current source and sink, through the network of conductor that is formed by the inclusions.

The conducting phase network can be described in terms of its global and its local properties. If the inclusions are spherical, then the global topological structure of the network can be identified with the Voronoi tessellation [53] generated by the centres of the inclusions. Two specimens have the same global topological structure if their associated Voronoi tessellations can be transformed into one another by translations, rotations, and dilations, without breaking and reforming any edges. A conductance is associated with each edge in the tessellation, and this conductance is a function of the inclusions that define the edge. A discrete version of the specimen can be constructed by assigning conductances to the edges of the tessellation in a particular specimen [54] and the effective conductance of this network can be found by using the methods of Doyle and Snell [40]. The effective conductance of a network of this sort is an example of a distance metric across a graph known as the resistance distance [55], and so ξ^{-1} is a continuous analogue of this metric for a network of conductor.

The structure of the global network will have a strong effect on the conductance of the specimen, which is constrained to lie between the Wiener bounds [56]. For a specimen with inclusion conductivity σ_1 and conducting phase conductivity σ_0, these bounds will be

$$\varsigma \leq p\sigma_1 + (1-p)\sigma_0 \tag{15}$$

$$\left(\frac{p}{\sigma_1} + \frac{1-p}{\sigma_0}\right)^{-1} \leq \varsigma \tag{16}$$

where p is the volume fraction of inclusions. For rectangular inclusions of the type shown in Figure 8 (left and centre), the lower and upper bounds hold exactly. In the central case, $1-p$ is also the fraction of A_1 available for charge to enter the specimen, and so for two square specimens of this type,

$$\frac{\varsigma_1}{\varsigma_2} = \frac{1-p_1}{1-p_2}.$$

This implies that for that particular geometry, the inclusions have a pure dilution effect, and the conductance is proportional to the amount of conductor present. If the geometry of the inclusions beyond A_1 does not consist of oriented rectangles that run through the specimen to A_0 (e.g. Figure 8, right), then the conductance will lie between the two bounds and will be approximately

$$\frac{\varsigma_1}{\varsigma_2} \approx \frac{1-p_1}{1-p_2} \times \frac{\xi_1}{\xi_2}. \tag{17}$$

The first term in (17) accounts for dilution, and the ratio of escape probabilities is a measure of tortuosity [57] adapted to DC conduction and similar transport processes.

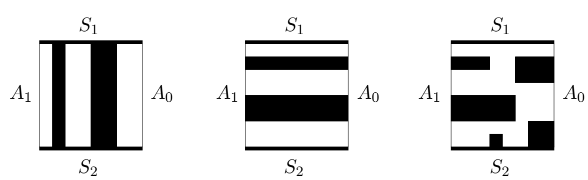

FIG. 8: For the specimen at left, the lower Wiener bound (15) holds exactly. For the centre specimen, the upper Wiener bound (16) holds exactly. For the specimen at right, its conductance lies between the two bounds.

By thinking of ξ^{-1} as a measure of distance, a contrast can be made with asymptotic approaches to conductance estimation. Suppose that the conductance of a specimen with inclusions is to be compared with the conductance of a specimen of pure conductor of the same size and shape. The Unsymmetric Effective Medium Approximation in this context yields a new specimen of a single phase whose conductivity lies between the Weiner bounds, and whose size, shape and conductance are the same as the original composite specimen.

In contrast, the methods developed here replace the specimen with one of pure conducting phase but different dimensions from the original. If no inclusions are present at A_1, the effect is to increase the length of the original inclusion free specimen by a factor of ϵ/ξ_c, where ξ_c is calculated for the composite specimen based on random walks starting from the line $x = \epsilon$. In this way, the methods developed here unravel the network structure of the particular specimen, and replace the topologically complex original specimen with a topologically trivial one having the same transport property.

VI. CONCLUSIONS

To summarize:

- The use of escape probabilities enables a conductance estimate to be made based on the structure of a particular given composite specimen.
- The procedure does not depend upon strong assumptions regarding internal specimen geometry or the dimensions of the problem, only that boundaries be reasonable and that they be known.
- The accuracy of the method can be controlled, and is only limited by computing capacity.
- The escape probabilities can be used to construct measures of tortuosity that are specifically suited to DC conductivity in materials that contain insulating inclusions.
- All results extend to specimens in $\mathbb{R}^3$.

Acknowledgments

Comments from Bruce Ankenman, Takeru Igusa, Alan Karr, Klaus Mecke, John Osborne, and Mark Freidlin were important in the development of the method. This research was funded in part by NSF grants DMS-9313013 and DMS-9208758 to the National Institute of

Statistical Sciences.

---

[1] J. Maxwell, *Treatise on Electricity and Magnetism* (Oxford UP, 1892), 3rd ed.

[2] S. Torquato, Appl. Mech. Rev. **44**, 37 (1991).

[3] V. Jikov, S. Kozlov, and O. Oleinik, *Homogenization of Differential Operators and Integral Functionals* (Springer, 1994).

[4] A. Sihvola, *Electromagnetic mixing formulas and applications* (IEE, 1999).

[5] L. Rayleigh, Philos. Mag. **34**, 481 (1892).

[6] I. Runge, Z. Tech. Phys. **6**, 61 (1925).

[7] R. McPhedran and D. McKenzie, Proc. R. Soc. London, Ser. A **359**, 45 (1978).

[8] R. O'Brien, J. Fluid Mech. **91**, 17 (1979).

[9] M. Zuzovksy and H. Brenner, Z. Angew. Math. Phys. **28**, 979 (1977).

[10] N. Harfield, J. Phys. D **32**, 1104 (1999).

[11] W. Perrins, D. McKenzie, and R. McPhedran, Proc. R. Soc. London, Ser. A **369**, 207 (1979).

[12] D. Bruggeman, Ann. Phys. (Leipzig) **24**, 636 (1935).

[13] R. Landauer, J. Appl. Phys. **23**, 779 (1952).

[14] R. Landauer, in *Electrical Transport and Optical Properties of Inhomogeneous Media*, edited by J. Garland and D. Tanner (AIP, 1978), pp. 2–43.

[15] C.-W. Nan, Prog. Mater. Sci. **37**, 1 (1993).

[16] Z. Hashin and S. Shtrikman, J. Appl. Phys. **33**, 3125 (1962).

[17] M. Beran, *Statistical Continuum Theories* (Wiley, New York, 1968).

[18] G. Milton, J. Appl. Phys. **52**, 5294 (1981).

[19] S. Torquato, J. Appl. Phys. **58**, 3790 (1985).

[20] A. Sen and S. Torquato, Phys. Rev. B **39**, 4504 (1989).

[21] G. Matheron, *Random Sets and Integral Geometry* (Wiley, 1975).

[22] D. Stoyan, W. Kendall, and J. Mecke, *Stochastic Geometry and its Applications* (Wiley, 1995), 2nd ed.

[23] G. Bánhegyi, Colloid. Polym. Sci. **264**, 1030 (1986).

[24] T. Hanai, in *Emulsion Science*, edited by P. Sherman (Academic, 1968), pp. 354–478.

[25] R. Turian, D. Sung, and F. Hsu, Fuel **70**, 1157 (1991).

[26] J. Petropoulos, J. Polym. Sci. Pol. Phys. **18**, 839 (1985).

[27] W. Kingery, J. Am. Ceram. Soc. **42**, 617 (1959).

[28] J. Dellimor and R. Gosling, J. Appl. Phys. **44**, 5599 (1973).

[29] H. Fricke, J. Phys. Chem. **57**, 934 (1953).

[30] D. Huntley, Can. J. Phys. **44**, 2952 (1966).

[31] Y. Baziard, S. Breton, S. Toutain, and A. Gourdenne, Eur. Polym. J. **24**, 512 (1988).

[32] G. Milton, Commun. Math. Phys. **99**, 463 (1985).

[33] R. Meredith and C. Tobias, J. Appl. Phys. **31**, 1270 (1960).

[34] C. Pearce, Br. J. Appl. Phys. **6**, 113 (1955).

[35] S. Chandrashekar, Rev. Mod. Phys. **15**, 2 (1943).

[36] P. De Gennes, La Recherche **7**, 919 (1976).

[37] D. Hong, H. Stanley, A. Coniglio, and A. Bunde, Phys. Rev. B **33**, 4564 (1986).

[38] O. Oleinik, A. Shimayev, and G. Yosifian, *Mathematical Problems in Elasticity and Homogenization* (North-Holland, 1992).

[39] D. Gilbarg and N. Trudinger, *Elliptic Partial Differential Equations of the Second Order* (Springer, 1983), 2nd ed.

[40] P. Doyle and J. Snell, *Random Walks and Electric Networks* (MAA, 1984).

[41] E. Garboczi and D. Bentz, J. Mater. Sci. **27**, 2083 (1992).

[42] H. Russell, J. Am. Ceram. Soc. **18**, 1 (1935).

[43] S. Cheung and R. Vachon, Int. J. Heat Mass Transfer **12**, 249 (1969).

[44] R. Crane and R. Vachon, Int. J. Heat Mass Transfer **20**, 711 (1977).

[45] M. Freidlin, *Functional Integration and Partial Differential Equations* (Princeton University Press, 1985).

[46] R. Bass, *Diffusions and Elliptic Operators* (Springer, 1998).

[47] J. Pickles, Proc. IEE **124**, 1271 (1974).

[48] M. Beasley, J. Pickles, G. d'Amico, M. Fanelli, M. Fanelli, G. Giusepetti, A. di Monaco, and G. Gallet, Proc. IEE **126**, 126 (1976).

[49] M. Muller, Ann. Math. Stat. **27**, 569 (1956).

[50] L. Schwartz and J. Banavar, Phys. Rev. B **39**, 11965 (1989).

[51] W. Press, S. Teukolsky, W. Vetterling, and B. Flannery, *Numerical Recipes in C* (Cambridge UP, 1992), 2nd ed.

[52] S. Karlin and H. Taylor, *A Second Course in Stochastic Processes* (Academic, 1981).

[53] A. Okabe, B. Boots, and K. Sugihara, *Spatial Tessellations: Concepts and Applications of Voronoi Diagrams* (Wiley, 1992).

[54] N. A. Vrettos, H. Imakoma, and M. Okazaki, J. Appl. Phys. **66**, 2873 (1989).

[55] D. Klein and M. Randic, J. Math. Chem. **12**, 81 (1993).

[56] O. Wiener, Abh. Math-Natur. Sächs. Akad. Wiss. **32**, 509 (1912).

[57] P. Carman, *Flow of Gases Through Porous Media* (Academic, 1956).